Cells and Materials

Volume 9 | Number 2 Article 2

1999

Effects of Casting Conditions and Annealing on Microstructures and Vickers Hardness of Dendritic Pd-Cu-Ga Dental Alloys

William A. Brantley
The Ohio State University

Qiang Wu
The Ohio State University

Zhuo Cai
The Ohio State University

Stanley G. Vermilyea
The Ohio State University

John C. Mitchell
The Ohio State University

See next page for additional authors

Effects of Casting Conditions and Annealing on Microstructures and Vickers Hardness of Dendritic Pd-Cu-Ga Dental Alloys

Authors

William A. Brantley, Qiang Wu, Zhuo Cai, Stanley G. Vermilyea, John C. Mitchell, and Michael C. Comerford

Cells and Materials Vol. 9, No. 2, 1999 (pages 83-92) 1051-6794/99$5.00+.25
Scanning Microscopy International, Chicago (AMF O'Hare), IL 60666 USA

EFFECTS OF CASTING CONDITIONS AND ANNEALING ON MICROSTRUCTURES AND VICKERS HARDNESS OF DENDRITIC Pd-Cu-Ga DENTAL ALLOYS

William A. Brantley[1,*], Qiang Wu[1,3], Zhuo Cai[1,4],
Stanley G. Vermilyea[1], John C. Mitchell[2] and Michael C. Comerford[2]

[1]College of Dentistry, [2]Materials and Chemical Analysis Research Center, Department of Geological Sciences, The Ohio State University, Columbus, OH 43210

(Received for publication April 30, 1998 and in revised form November 2, 1998)

Abstract

Three Pd-Cu-Ga alloys with as-cast dendritic microstructures and very similar compositions, two containing less than 1 wt% boron and the third boron-free, were cast with normal bench-cooling or rapid-quenching into water. Quenched specimens were also heat treated at temperatures of 1000°, 1200°, 1500° and 1800°F that span the firing cycles for dental porcelain. Similar values of Vickers hardness were observed for all three alloys, suggesting little effect from boron on yield strength. The hardness was relatively insensitive to the experimental conditions, except for heat treatment at 1500° and 1800°F where significant softening occurred with transformation of the microstructure to Pd_2Ga and the palladium solid solution.

Key Words: Palladium, dental alloy, solidification, microstructure, dendritic, eutectic, scanning electron microscopy, Vickers hardness, heat treatment.

[3]Present address: Therm-O-Disc, Inc., Mansfield, OH 44907
[4]Present address: Department of Biomaterials Science, Baylor College of Dentistry, Texas A & M University System, Dallas, TX 75246

*Address for Correspondence:
William A. Brantley
Section of Restorative Dentistry, Prosthodontics and Endodontics, College of Dentistry
The Ohio State University
305 West 12th Avenue
Columbus, Ohio 43210-1241
Telephone Number: (614) 292-0773
FAX Number: (614) 292-9422
E-mail: brantley.1@osu.edu or
wbrantle@columbus.rr.com

Introduction

The Pd-Cu-Ga dental alloys containing about 10 weight% (wt%) Cu and 6-9 wt% Ga date from the patent by Schaffer (1983) for the Option alloy (Ney Dental, Bloomfield, CT). The introduction of these alloys subsequently led to the development of a variety of other high-palladium dental alloys containing > 70 wt% Pd by the manufacturers. These alloys have been used for metal-ceramic restorations (Carr and Brantley, 1991) and implant-supported prostheses (Stewart *et al.*, 1992). Some of the as-cast Pd-Cu-Ga alloys lack grain-refining elements (typically ruthenium) and have a dendritic as-cast structure (Brantley *et al.*, 1993). Cast restorations with this dendritic microstructure may experience "hot tears" (microscopic fractures at elevated temperature) along the interdendritic regions during the recommended bench-cooling after casting, particularly in thin sections where there is insufficient metal to provide support (Carr *et al.*, 1993). The dendritic Pd-Cu-Ga alloys remain popular clinically, particularly for implant-supported prosthesis applications where there is ample supporting metal. The relatively high values of elastic modulus and yield strength of these alloys provide excellent flexural rigidity and resistance to permanent deformation for long-span applications.

The present research had the following objectives: (a) to determine whether the rate of solidification during casting significantly affects the microstructures and Vickers hardness of three dendritic as-cast Pd-Cu-Ga alloys having very similar compositions; (b) to investigate whether use of a post-casting heat treatment over a temperature range spanning the porcelain firing cycles affected the microstructures and Vickers hardness of the three alloys in different manners; (c) to establish whether the presence of boron in the alloy composition significantly affects the microstructures and Vickers hardness. The incorporation of boron in high-palladium alloys is thought to modify the properties of the grain boundary regions (Carr and Brantley, 1991), and to provide some hardening and strengthening (van der Zel, 1989). Boron

is also considered to serve as a scavenger for oxygen when the alloy is melted and thus to provide some protection against the undesired incorporation of oxides in the cast alloy (van der Zel, 1989). This work is an extension of a recent study (Brantley *et al.*, 1996) that compared the effects of similar solidification rates and heat-treatment temperatures on the Vickers hardness of one of these dendritic as-cast Pd-Cu-Ga alloys and a second Pd-Cu-Ga alloy with a fine-grained as-cast microstructure containing a near-surface eutectic constituent.

Materials and Methods

Three Pd-Cu-Ga alloys of nominal composition 79Pd-10Cu-9Ga-2Au were selected for study. Two alloys (Option; Spartan, Williams/Ivoclar, Amherst, NY) have identical compositions as provided by the manufacturers and contain small proprietary amounts (< 1 wt%) of boron. The third alloy (Spartan Plus, Williams/Ivoclar) is boron-free but otherwise has the same composition as Spartan (S.P. Schaffer, Williams/Ivoclar, private communication).

Castings simulating a maxillary incisor coping and cast plate-shaped specimens having dimensions of 20 mm x 20 mm x 1.5 mm were prepared using previously described procedures (Carr and Brantley, 1991). The bench-cooling recommended by the manufacturers was employed after casting (ACBC condition), as well as rapid-quenching after casting (ACRQ condition) to better retain the elevated-temperature microstructure for subsequent heat-treatment experiments (Brantley *et al.*, 1996). The quenched specimens were heat treated (Mark IV Digital Furnace, Ney Dental) for 10 minutes at temperatures of 1000°, 1200°, 1500° and 1800°F, which span the firing cycle temperature range (Papazoglou *et al.*, 1993) for Vita VMK dental porcelain (Vident, Baldwin Park, CA), followed by quenching in water. Some quenched specimens were also subjected to prolonged periods (1 to 5 hours) of heat treatment at 1800°F, also followed by quenching in water. For comparison, the bench-cooled specimens were subjected to heat treatment simulating the complete porcelain firing cycles (Ultra-Mat Digital Furnace, Unitek Corp, Monrovia, CA).

Cross-sectioned simulated-coping specimens were subjected to standard metallographic polishing procedures through 0.05 μm alumina slurries and etched in aqua regia solutions. The laboratory procedure for cross-sectioning the specimens has been described previously (Brantley *et al.*, 1996). Microstructures of these etched specimens were observed with a scanning electron microscope (SEM; JEOL JSM-820, JEOL Ltd., Tokyo, Japan). All of the presented micrographs are secondary electron images. Vickers hardness measurements were performed on two cross-sectioned and etched specimens (N = 10) for each alloy condition, using a 1 kg load and 30 seconds dwell time, to assess the effects of the solidification rates and heat treatments on the overall mechanical properties of the three alloys. The 1 kg load yielded indentations that covered both dendritic and interdendritic regions to yield an average hardness for each alloy specimen. In addition, the microhardness values of the dendrites and interdendritic regions for two cross-sectioned and etched specimens of each alloy in the bench-cooled condition (ACBC) were obtained using a 10 g load and the same dwell time (N = 10). This light load yielded sufficiently small indentations that the microhardness values of the separate dendritic and interdendritic regions in the specimens could be measured.

The hardness data were analyzed statistically using analysis of variance (ANOVA) and the Ryan-Einot-Gabriel-Welsch (REGW) tests for multiple comparisons of means. The REGW test is considered more powerful than the conventional Tukey multiple range test, with less possibility of type II (false negative) statistical errors (Welsch, 1977). A level of $\alpha = 0.01$ was selected for statistical significance. The two statistical analyses were performed simultaneously on all solidification and heat-treatment conditions of the three alloys, because of their nearly identical compositions, rather than performing the analyses on each of the three alloys individually.

Quantitative chemical composition information was provided by energy-dispersive x-ray spectroscopic (EDS) spot analyses at selected sites (N = 5) in the microstructures of carbon-coated cross-sectioned (etched) specimens. EDS was performed using a Link eXL microanalysis system with a PentaFet detector and an ultrathin window (Oxford Instruments Group, High Wycombe, England).

X-ray diffraction (XRD) analyses were obtained at room temperature from the surfaces of the polished and etched, plate-shaped specimens (not cross-sectioned) of the Option and Spartan Plus alloys in the different treatment conditions. An x-ray diffractometer (PAD-V, Scintag, Sunnyvale, CA) was used with a diffraction angle (2θ) range from 30° to 100°, a scanning rate of 0.5° per minute and Cu Kα radiation to qualitatively reveal the different microstructural phases.

Electron microprobe analysis (SX-50, Cameca, Paris, France) was employed to investigate the presence of boron in the microstructures of etched cross-sectioned specimens of the Spartan and Option alloys. Linescans, spot analyses, raster scans and dot mapping techniques were used to examine the bulk dendrites, the boundaries between the dendrites and interdendritic regions, and the interdendritic regions for representative as-cast and bench-cooled specimens of the three alloys.

Table 1. Vickers hardness of the high-palladium alloys for different solidification and heat-treatment conditions.

Alloy	ACBC	ACRQ	ACRQ and 1000°F HT	ACRQ and 1200°F HT	ACRQ and 1500°F HT	ACRQ and 1800°F HT	ACBC and PFC
Spartan	349 ± 18 BCDE	378 ± 12 ABC	390 ± 9 A	347 ± 15 BCDE	308 ± 8 FG	288 ± 5 G	314 ± 7 G
Spartan Plus	354 ± 14 BCD	351 ± 6 BCD	379 ± 14 AB	363 ± 22 ABC	319 ± 6 EFG	290 ± 11 G	296 ± 8 G
Option	348 ± 10 BCDE	346 ± 10 CDE	357 ± 7 BCD	328 ± 5 DEF	296 ± 6 G	288 ± 5 G	292 ± 12 G

ACBC: As-cast and bench-cooled. ACRQ: As-cast and rapidly-quenched.

ACRQ and 1000°F HT, 1200°F HT, 1500°F HT, and 1800°F HT: ACRQ and heat treated at 1000, 1200, 1500 and 1800°F, respectively.

ACBC and PFC: ACBC and subjected to simulated porcelain firing cycles (Papazoglou *et al.*, 1993).

Hardness measurements (N = 10) were performed using 1 kg load and 30 seconds dwell time. Mean values in both the columns and the rows with the same letter code for the REGW analysis are not significantly different (P > 0.01). Results for all solidification and heat-treatment conditions for the three alloys were compared at the same time, rather than performing a separate statistical analysis for each alloy.

Table 2. Vickers hardness of different phases in the interdendritic and dendritic areas for the Option and Spartan Plus alloys in three different treatment conditions.

Condition	Option Alloy Interdendritic Region: Secondary Phase Particles	Spartan Plus Alloy Interdendritic Region: Secondary Phase Particles	Option Alloy Dendritic Region: Palladium Solid Solution	Spartan Plus Alloy Dendritic Region: Palladium Solid Solution
ACBC	419 ± 25 B	451 ± 19 A	259 ± 9 D	257 ± 12 D
ACRQ 1200°F HT	357 ± 15 C	430 ± 23 AB	250 ± 9 D	269 ± 10 D
ACRQ 1800°F HT	364 ± 16 C	361 ± 17 C	259 ± 9 D	250 ± 15 D

Hardness measurements (N = 10) were made using a 10 gm load and a 30 seconds dwell time. Mean values in both the columns and the rows with the same letter code for the REGW analysis are not significantly different (P > 0.01).

Results

The mean Vickers hardness values of the three Pd-Cu-Ga alloys for the different experimental conditions are listed in Table 1 (it should be recalled that the ANOVA and REGW tests were performed simultaneously on all solidification and heat-treatment conditions of the three alloys, rather than the results for each alloy being analyzed separately.) There was no significant difference when the mean hardness values of each alloy were compared for the as-cast bench-cooled (ACBC) and as-cast rapidly-quenched (ACRQ) conditions. While 1000°F is the hardening temperature recommended by the manufacturers, there was no significant difference in the hardness for each alloy after heat treatment at this temperature compared to either the ACBC or ACRQ condition, other than for ACBC Spartan. For the Spartan alloy, heat treatment at 1200°F caused a significant decrease in hardness compared to heat treatment at 1000°F, but a significant decrease was not observed for the Spartan Plus and Option alloys. For all three alloys, there was a significant decrease in hardness when the

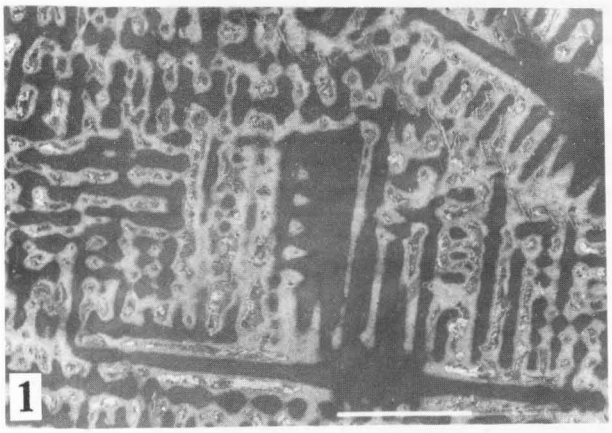

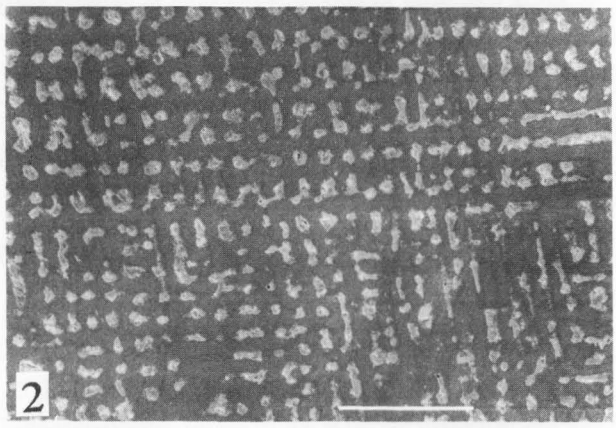

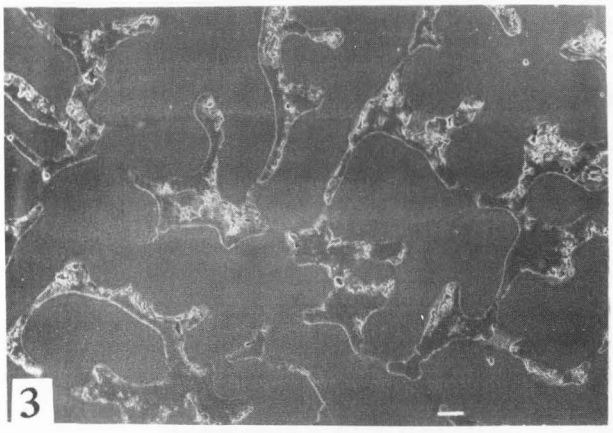

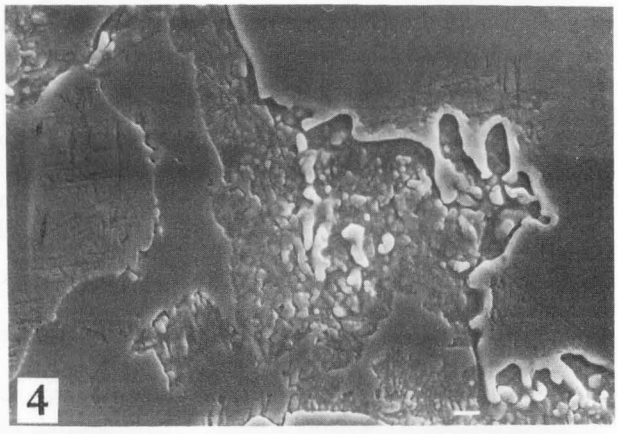

Figure 1. Microstructure of as-cast and bench-cooled (ACBC) Spartan. The dendritic structure is evident. Bar = 100 μm.

Figure 2. Microstructure of as-cast and rapidly-quenched (ACRQ) Spartan. The dendritic structure is much finer compared to Figure 1. Bar = 100 μm.

Figure 3. Microstructure of ACRQ Spartan Plus, showing the dendritic structure at a substantially higher magnification than used for Figure 2. Bar = 10 μm.

Figure 4. High-magnification photomicrograph of ACRQ Spartan Plus, showing complex interdendritic regions and areas of needle-shaped Widmanstätten precipitates in the dendrites. For this somewhat overetched specimen, it is difficult to determine whether some microstructural features in the interdendritic regions are secondary phase particles or etching patterns of a eutectic constituent. Bar = 1 μm.

heat-treatment temperature was increased from 1200° to 1500°F, but there was no significant difference in hardness for heat treatment at temperatures of 1500° and 1800°F. There was also no significant difference in hardness after heat treatment at 1800°F, compared to that after the simulated complete porcelain firing cycles for the three alloys.

Table 1 also shows that, other than after heat treatment at 1000°F, there was no significant difference in the hardness of the boron-containing Spartan and Option alloys, which contain the same nominal percentages of Pd, Cu and Ga. Moreover, there was no significant difference in hardness for Spartan and the boron-free Spartan Plus alloy for any of the solidification and heat-treatment conditions investigated. In practice, it is doubtful that a variation of 10% or less in hardness would have any practical significance for an alloy in the dental laboratory, and Table 1 indicates that little meaningful change in hardness occurred until a heat-treatment temperature of 1500°F was used.

Mean hardness values of the dendrites (palladium solid solution matrix) and the secondary phase particles in the interdendritic regions for Option and Spartan Plus (to be discussed later) are listed in Table 2 for three

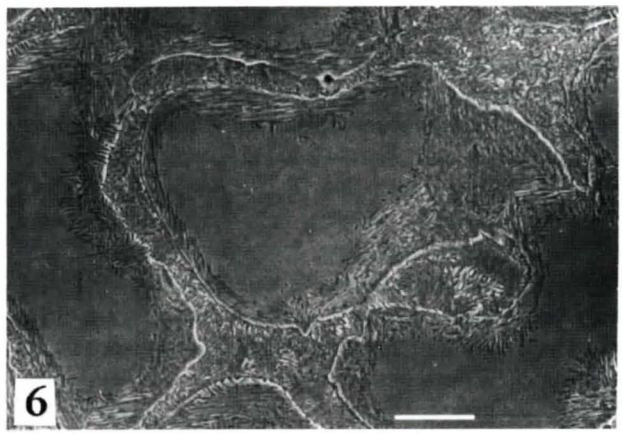

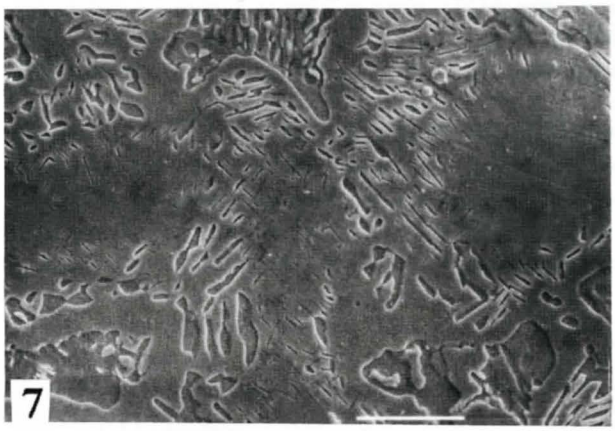

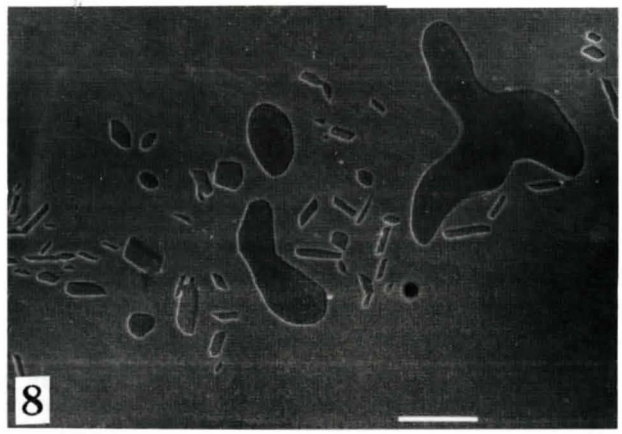

Figure 5. High-magnification photomicrograph of ACBC Spartan Plus. Widmanstätten precipitates in the dendrites and embedded particles in the interdendritic region can be clearly seen. As in Figure 4, the particles may be a secondary phase or the etching pattern of a eutectic constituent. Bar = 1 μm.

Figure 6. Microstructure of ACRQ Spartan Plus after heat treatment at 1200°F. Complex discontinuous precipitates have formed around the interdendritic regions. Bar = 10 μm.

Figure 7. Microstructure of ACRQ Spartan Plus after heat treatment at 1500°F. The original as-cast dendrites have begun to disappear, and new secondary phases have formed. Bar = 10 μm.

Figure 8. Microstructure of ACRQ Spartan Plus after heat treatment at 1800°F. The original dendritic microstructure has disappeared, and secondary phases of different morphologies have formed in the palladium solid solution matrix. Bar = 10 μm.

---

experimental conditions. There is a considerable difference in the hardness of this interdendritic constituent and the dendrites for both alloys, showing the substantial contribution of the interdendritic regions to the overall alloy hardness. There was no significant difference in the hardness of the dendrites for the two alloys and the three experimental conditions. The hardness of the secondary phase particles in the interdendritic regions was highest for Spartan Plus in the ACBC condition, but not significantly different for this alloy after heat treatment at 1200°F. However, the hardness of the interdendritic region in Option was significantly lower after heat treatment at 1200°F compared to the ACBC condition. There was no significant difference in the hardness of the interdendritic constituent in Option after heat treatments at 1200° and 1800°F, although there was a considerable decrease in hardness of this constituent in Spartan Plus after the higher heat-treatment temperature.

Figures 1 and 2 are photomicrographs of Spartan in the ACBC and ACRQ conditions, respectively. It can be seen that the rapid quenching has reduced the scale of the as-cast dendritic microstructure, although there is no significant difference in the Vickers hardness for the two solidification conditions. The same result was observed

for the Option and Spartan Plus alloys, and has been previously reported (Brantley *et al.*, 1996).

Figures 3 and 4 show the microstructure of ACRQ Spartan Plus at higher magnifications (the microstructures of Spartan and Spartan Plus are very similar.) In Figure 4, it is assumed that the somewhat overetched complex interdendritic regions may contain a lamellar eutectic constituent similar to that shown previously for the ACBC Spartan (Brantley *et al.*, 1993) and Spartan Plus (Brantley *et al.*, 1995) alloys. Other microstructural features are assumed to be hard secondary phase particles, as discussed later; also, areas of needle-shaped Widmanstätten precipitates can be seen. Figure 5 reveals that there is a higher density of the Widmanstätten precipitates for the ACBC condition of this alloy, and embedded particles in the interdendritic region are evident in the center of the figure. These may be particles of some secondary phase as well as the etching pattern of a fine-scale eutectic constituent.

After heat treatment at 1200°F, complex discontinuous precipitate structures were observed in all three alloys around the interdendritic regions (Figure 6). When the heat-treatment temperature was increased to 1500°F, the dendritic structure began to disappear, and intermediate phases of several morphologies formed from the interdendritic regions and discontinuous precipitates, as shown in Figure 7. At low magnification, the correspondence between the locations of these secondary phases and the orientation of the original dendritic structure was evident. With periods of up to 5 hours heat treatment at 1800°F for all three alloys, the amount of the smaller secondary phase decreased slightly, while the larger secondary phase retained the rounded morphology (Figure 8).

The stable larger secondary phase that appeared after heat treatment at 1800°F (Figure 8) had a similar morphology in all three alloys. Representative EDS analyses for the Option alloy indicated that this phase had a composition of 67.3 $\pm$ 0.4 Pd, 15.6 $\pm$ 0.3 Cu and 16.5 $\pm$ 0.5 Ga (values in atomic %). Assuming that the copper atoms occupy the gallium sites (Odén and Herø, 1986), this composition would correspond approximately to Pd_2Ga. EDS analyses were not performed on the smallest secondary phase particles (approximately 1-2 μm width) in Figure 8, but it is tentatively hypothesized that these particles are also Pd_2Ga.

X-ray diffraction patterns are presented in Figures 9 and 10 for different experimental conditions of the Option and Spartan Plus alloys, respectively. Interpretation of these XRD patterns is facilitated by comparison to a previously published XRD pattern for ACBC Spartan Plus (Brantley *et al.*, 1995). The relative intensities of the {111}, {200}, {220}, {311} and {222} peaks for the palladium solid solution matrix are considerably different from those of the ICDD (International Center for Diffraction Data, Swarthmore, PA) powder standard for palladium because of the strong preferred orientation of the palladium solid solution dendrites in these cast alloys (Brantley *et al.*, 1995). For example, the {220}, {311} and {222} peaks for the palladium solid solution in the ACBC Option alloy cannot be seen in Figure 9, although a strong {311} peak and a weak {222} peak were observed for the ACRQ condition. For ACBC Spartan Plus in Figure 10, the {220} and {311} peaks for the palladium solid solution were not present for the ACBC condition, while a weak {222} peak was found. This latter peak largely disappeared for ACRQ Spartan Plus, and weak {220} and {311} peaks were observed. A strong {220} peak for the palladium solid solution in Spartan Plus was observed after heat treatment at 1200°F, and this peak was very strong after heat treatment at 1800°F for the specimen examined.

Figures 9 and 10. X-ray diffraction patterns for the Option (**Fig. 9, facing page, top**) and Spartan Plus (**Fig. 10, bottom**) alloys in the ACBC and ACRQ conditions, and after heat treatment at 1200° and 1800°F.

Identification of peaks attributed to Pd_2Ga is based upon (a) previous XRD patterns (Brantley *et al.*, 1995) for the as-cast Spartan Plus alloy and for the as-cast Pd-Cu-Ga alloy Liberty which contains predominantly a near-surface eutectic constituent consisting of Pd_2Ga and the palladium solid solution, and (b) the new version of the Pd-Ga phase diagram published by the American Society for Metals (Massalski, 1990), as discussed below. Other XRD peaks that are observed in Figures 9 and 10 for the alloys in the ACBC and ACRQ conditions and after heat treatment at 1200°F are tentatively indexed to the Pd_5Ga_2 and $Pd_{13}Ga_5$ phases in the new version of the Pd-Ga phase diagram (Massalski, 1990), as will be discussed later.

Extensive examination with the electron microprobe failed to detect boron in the interdendritic regions or within the dendrites of the as-cast and bench-cooled Option and Spartan alloys.

Discussion

The present results demonstrate that the Vickers hardness, and presumably the yield strength (Dieter, 1986), for Option, Spartan and Spartan Plus are very similar, when the alloys are subjected to the same solidification and heat-treatment conditions. Schaffer (private communication) has suggested that boron might have a deleterious effect on the high-temperature creep or distortion characteristics of these Pd-Cu-Ga alloys, which is the reason that this element is not included in the composition of Spartan Plus.

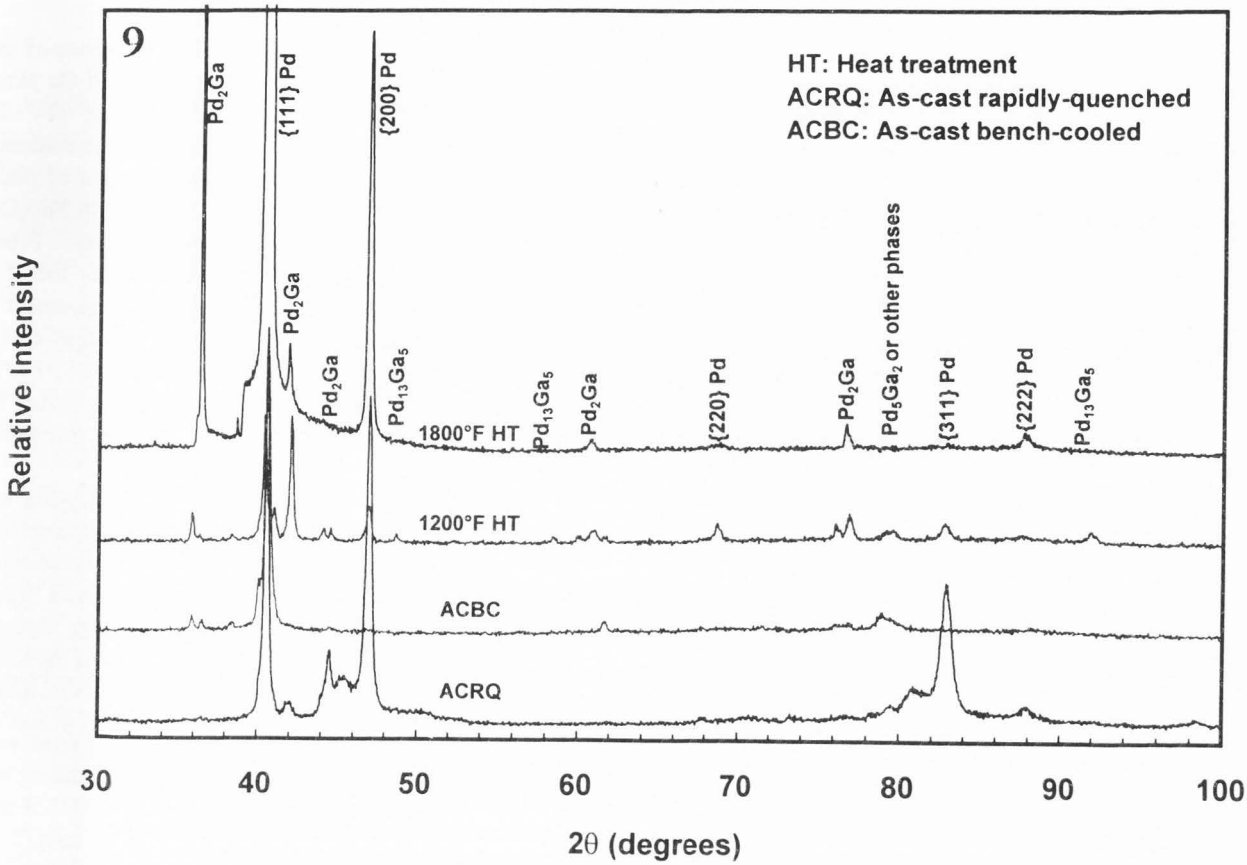

Figures 9 and 10 here

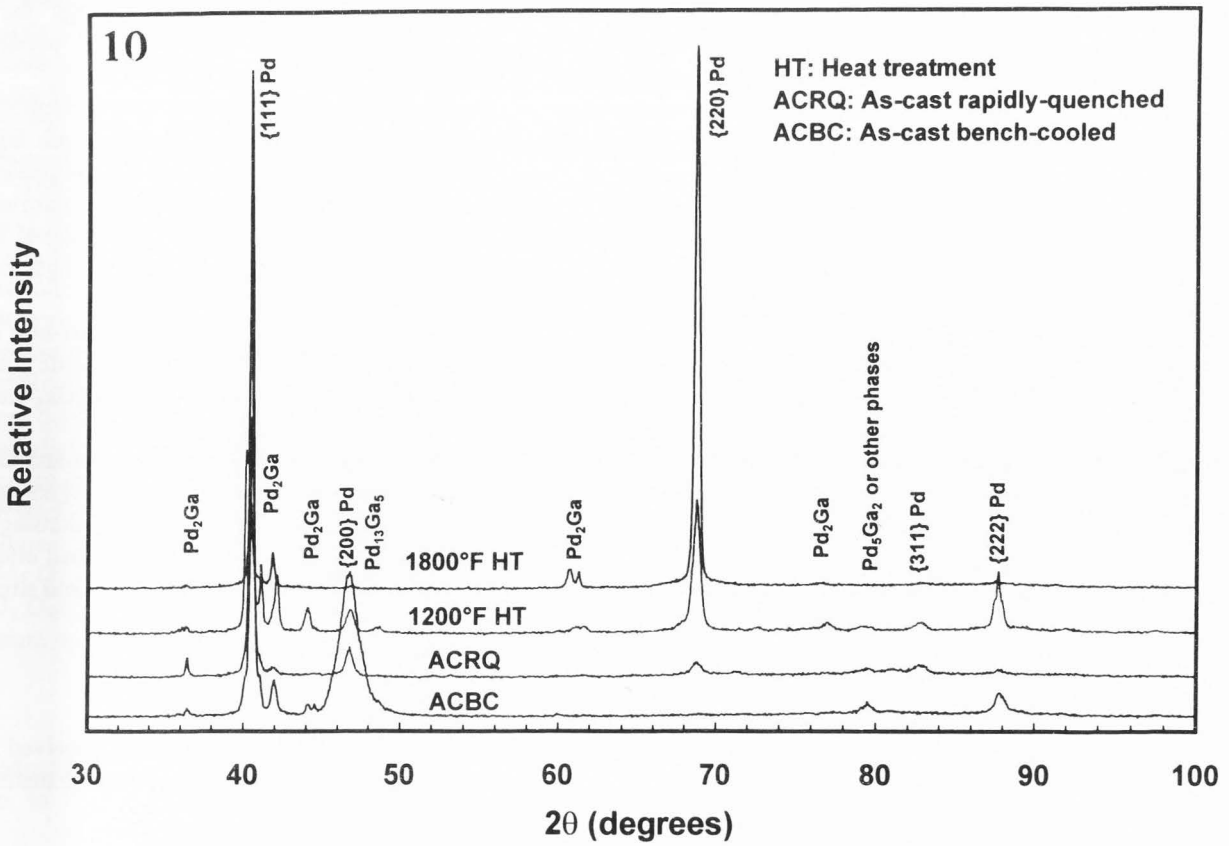

While cast dental alloys are known to undergo rapid solidification because of the large difference between the temperatures of the molten alloy and investment, Figures 1 and 2 clearly show that rapid quenching following solidification significantly affects the scale of the as-cast dendritic structure (Brantley *et al.*, 1996). This is attributed to kinetic effects associated with the much more limited time available for atomic diffusion and solute redistribution, which also resulted in the reduced density of Widmanstätten precipitates when the alloy was rapidly quenched after casting (Brantley *et al.*, 1996).

The complex interdendritic regions of these as-cast alloys contain particles of a secondary phase (Figures 4 and 5), which is assumed to account for their greater hardness compared to the palladium solid solution dendrites (Table 2). The relatively high hardness of the Pd-Cu-Ga alloy Liberty (Jelenko, Armonk, NY) has been shown to arise from the presence of a hard secondary phase, tentatively interpreted as Pd_5Ga_2 (Wu *et al.*, 1997), rather than the network of submicron face-centered tetragonal $Pd_3Ga_xCu_{1-x}$ precipitates previously proposed by Odén and Herø (1986). Transmission electron microscopic studies (Cai *et al.*, 1997) have established that the tweed structure observed by Odén and Herø (1986) in a Pd-Cu-Ga alloy with a composition similar to that of Spartan, was present in the Liberty and Spartan Plus alloys and two Pd-Ga alloys. This confirmed that the tweed structure does not account for the higher hardness of the Liberty and Spartan Plus alloys. The differences in hardness for the interdendritic regions compared to the palladium solid solution dendrites for the three Pd-Cu-Ga alloys in the present study are attributed to the presence of this hard phase (presumably Pd_5Ga_2) in the interdendritic regions. The very small size of the secondary phase particles in Figures 4 and 5 precluded accurate determinations of their composition using EDS analyses. The decrease in hardness of the alloys after heat treatments at 1500° or 1800°F (Table 1) may arise from transformation in the ultrastructure at the transmission electron microscopic level or in the microstructural transformations observed with the SEM.

Considering the composition of the three Pd-Cu-Ga alloys and the Pd-Ga phase diagram (Massalski, 1990), the equilibrium phases at 1800°F should be the palladium solid solution and the Pd_2Ga phase. As previously noted, EDS analysis suggested that the composition of the large, rounded secondary phases in the alloy specimens heat treated at 1800°F corresponded to Pd_2Ga. Moreover, Figures 9 and 10 show that the Pd_2Ga phase was found in all of the other experimental conditions investigated for these alloys and had an extreme preferred orientation in the Option alloy specimen heat treated at 1800°F. Tentative assignment of a peak near 80° to Pd_5Ga_2 for ACBC Option (Figure 9) and ACBC Spartan Plus (Figure 10) follows from the likely presence of this phase in the as-cast alloys, based upon the Pd-Ga phase diagram (Massalski, 1990), although this peak may also arise from other phases such as Pd_2Ga and the Widmanstätten precipitates. Likewise, the assignment of peaks from the specimens heat treated at 1200°F to $Pd_{13}Ga_5$ is also based upon the Pd-Ga phase diagram. Previously, the complex discontinuous precipitates found in four other high-palladium alloys after heat treatment at 1200°F were interpreted as alternating lamellae of the palladium solid solution and $Pd_{13}Ga_5$ (Wu *et al.*, 1997). Planned XRD analyses of model binary alloys having the compositions of Pd_2Ga, Pd_5Ga_2 and $Pd_{13}Ga_5$ are necessary to verify these hypotheses.

Lastly, failure to detect boron in the Option and Spartan alloys is not surprising, since both alloys contain less than 1 wt% of this element. Evidently, microsegregation during solidification to yield locally much higher boron concentrations at sites such as boundaries between dendrites and interdendritic regions, or within the interdendritic regions, does not occur. Another possibility is loss of boron during fusion of the alloy (S.P. Schaffer, private communication).

Conclusions

(1). The three Pd-Cu-Ga alloys studied (Spartan, Spartan Plus and Option) exhibited very similar microstructures and values of Vickers hardness for the different solidification and heat-treatment conditions investigated.

(2). With increasing heat-treatment temperature from 1000° to 1800°F, the Vickers hardness significantly decreased. This is attributed to the disappearance of the dendritic as-cast microstructure and transformation of the Pd_5Ga_2 hard phase, which is considered to be responsible for the high hardness and strength of the Pd-Cu-Ga alloys.

(3). The secondary phase remaining after heat treatment of the alloys at 1800°F is Pd_2Ga, while the discontinuous precipitates may consist of $Pd_{13}Ga_5$ and the palladium solid solution.

(4). Boron was not detected in Spartan and Option by the electron microprobe because of its low concentration and apparent absence of appreciable microsegregation. This small amount of boron has minimal effect on the Vickers hardness (and presumably the yield strength) of these alloys.

Acknowledgment

Support for this investigation was received from Research Grant DE10147 from the National Institute of Dental Research, Bethesda, MD 20892.

References

Brantley WA, Cai Z, Carr AB, Mitchell JC (1993) Metallurgical structures of as-cast and heat-treated high-palladium dental alloys. Cells Mater **3**, 103-114.

Brantley WA, Cai Z, Foreman DW, Mitchell JC, Papazoglou E, Carr AB (1995) X-ray diffraction studies of as-cast high-palladium alloys. Dent Mater **11**, 154-160.

Brantley WA, Cai Z, Vermilyea SG, Papazoglou E, Mitchell JC, Carr AB (1996) Effects of solidification conditions and heat treatment on the microstructure and Vickers hardness of Pd-Cu-Ga dental alloys. Cells Mater **6**, 127-135.

Cai Z, Brantley WA, Clark WAT, Colijn HO (1997) Transmission electron microscopic investigation of high-palladium dental casting alloys. Dent Mater **13**, 365-371.

Carr AB, Brantley WA (1991) New high-palladium casting alloys: Part 1. Overview and initial studies. Int J Prosthodont **4**, 265-275.

Carr AB, Cai Z, Brantley WA, Mitchell JC (1993) New high-palladium casting alloys: Part 2. Effects of heat treatment and burnout temperature. Int J Prosthodont **6**, 233-241.

Dieter GE (1986) Mechanical Metallurgy (3rd ed.). McGraw-Hill, New York. pp. 329-332.

Massalski TB (Editor-in-Chief) (1990) Binary Alloy Phase Diagrams (2nd ed.), Vol. 2. ASM International, Materials Park, OH. pp. 1836 and 1838.

Odén A, Herø H (1986) The relationship between hardness and structure of Pd-Cu-Ga alloys. J Dent Res **65**, 75-79.

Papazoglou E, Brantley WA, Carr AB, Johnston WM (1993) Porcelain adherence to high-palladium alloys. J Prosthet Dent **70**, 386-394.

Schaffer SP (1983) Novel palladium alloy and dental restorations utilizing same. US Patent 4,387,072.

Stewart RB, Gretz K, Brantley WA (1992) A new high-palladium alloy for implant-supported prostheses. J Dent Res **71**, 158 (AADR Abst. no. 423).

van der Zel JM (1989) High-Temperature Behavior of Palladium-Based Dental Alloys. Doctoral Thesis, University of Amsterdam, Netherlands.

Welsch RE (1977) Stepwise multiple comparison procedures. J Amer Stat Assoc **72**, 566-575.

Wu Q, Brantley WA, Mitchell JC, Vermilyea SG, Xiao J, Guo W (1997) Heat-treatment behavior of high-palladium dental alloys. Cells Mater **7**, 161-174.

Discussion with Reviewers

H.J. Mueller: If bench cooling of Pd-Cu-Ga alloys is known to produce "hot tears" along interdendritic regions, then rapid quenching should be more severe in this regard. Were "hot tears" detected with any of the quenched samples prepared in this study? If not, then hot tearing may not be much of a problem with these alloys.

Authors: While not a focus of the present study, hot tears will be more severe in the rapidly quenched specimens of these three alloys, compared to specimens that are bench cooled, as previously reported by Brantley *et al.* (1996).

H.J. Mueller: From the results from this study, it may be inferred that samples that are rapidly quenched after casting (ACRQ) and heat treated at 1800°F will have about the same hardness as samples that are bench cooled after casting and then subjected to the porcelain firing cycles. Will bonding to porcelain be different between these two types of samples due to the vast microstructural differences?

Authors: Further research is required in order to answer this question, since the porcelain adherence is expected to be significantly influenced by the complex near-surface oxide structure found in these alloys (Brantley *et al.*, 1996b). This oxide structure may differ for the present heat treatment at 1800°F, compared to that after the complete porcelain firing cycles.

M.D. Bagby: Why do you assume that Cu occupies Ga sites in Pd_2Ga when the Pd-Cu binary phase diagram shows that Pd and Cu are miscible in the solid state (although a superlattice region is also shown)?

Authors: We have followed the convention of Odén and Herø (1986), who previously assigned Cu to Ga sites when hypothesizing the solid-state peritectoid transformation of the palladium solid solution to a submicron $Pd_3Ga_xCu_{1-x}$ precipitate structure. With the assumption that Cu occupies the Ga sites, our interpretation that the precipitates in the alloy specimens heat treated at 1800°F are Pd_2Ga is consistent with the form of the Pd-Ga phase diagram currently approved by the American Society for Metals (Wu *et al.*, 1997).

M.D. Bagby: What effects did etching the samples have on the EDS and XRD results? Could etching have removed boron from the surface?

Authors: Our previous experience (Brantley *et al.*, 1993) has been that etching does not greatly affect the EDS results with the SEM for the major elements in the high-palladium alloys. While surface boron might be removed by such etching, we assumed that subsurface boron would be detected with the much greater beam current densities used with the microprobe. We agree that additional research is needed to locate the boron in the Spartan and Option alloys (and to verify its absence

in Spartan Plus below instrumental detection limits). The specimens for XRD analyses were etched to remove the permanently deformed surface layer resulting from metallographic polishing. We have found with dental alloys that this procedure yields sharper XRD peaks. In previous research (Brantley *et al.*, 1995), where the as-cast Pd-Ga alloy Protocol (Williams/Ivoclar) was examined by XRD in the unetched and etched conditions, there was little difference in the XRD patterns, despite the presence of a grain-boundary precipitate. Consequently, we do not expect that the use of unetched specimens would have yielded substantially different XRD results.

Additional Reference

Brantley WA, Cai Z, Papazoglou E, Mitchell JC, Kerber SJ, Mann GP, Barr TL (1996b) X-ray diffraction studies of oxidized high-palladium alloys. Dent Mater **12**, 333-341.